ISSN: 0067-2904

Synthesis and Characteristics of Ag, Cu/Au Core/Shell Nanoparticles Produced by Pulse Laser Ablation

Isam M. Ibrhim
Department of Physics, College of Science, University of Baghdad, Baghdad, Iraq.

Abstract

Colloidal dispersions of mono Au, Ag , Cu and bimetallic Ag/Au and Cu/Au core/shell nanoparticles are synthesized by pulsed laser ablation of metals targets immersed in 5 ml distilled water (DW). Surface Plasmon resonance (SPR) and particle sizes are characterized by UV-VIS and HRTEM, the X-ray diffraction shows the structure of core/shell. The Surface Plasmon resonance of the produced nanoparticles solutions for silver nanoparticles about 402 nm and copper nanoparticles about 636 nm. While for the core-shell observed two peaks of SPR, Ag/Au core/shell at (406-516) nm, and Cu/Au core/shell observed one peak at 565nm, because the region of gold and copper close together. The shape and particle size have been confirmed by HRTEM measurement, average size is around 12nm for Ag NPs, and 14nm for Cu NPs, while the average size is around 11nm for Ag/Au core/shell NPs and around 13nm for Cu/Au core/shell NPs. Zeta potential (ZP) results proved the silver nanoparticle is more stabilizing (-23.11 mV) than other noble metal nanoparticles,while Ag/Au core/shell is more stabilizing(-27.77mV) with comparison with Cu/Au core/shell which less stabilizing.

Keywords: Noble metal nanoparticles (NMNPs), surface Plasmon resonance (SPR), pulse laser ablation in liquid (PLAL), Zeta Potential (ZP),

تحضير وخصائص الجسيمات النانوية ل Ag,Cu/Au (لب– قشرة) المستحصلة بواسطة استئصال الليزر النبضي

عصام محمد ابراهيم
قسم الفيزياء، كلية العلوم، جامعة بغداد، بغداد، العراق.

الخلاصة

تم تحضير السائل الغروي للعناصر Au، Ag و Cu والمعادن الثنائية Ag/Au و Cu/Au (لب/قشرة) للجسيمات النانوية بطريقة الليزر النبضي لاقراص هذه المعادن المغموره في 5ml من الماء المقطر . تم اجراء فحوصات طيف UV–VIS وفحوصات الاشعة السينية لايجاد التركيب البلوري ل(لب/قشرة)، وكذلك فحوصات المجهر الالكتروني النافذ ذو الدقة العالية (HRTEM) لحساب حجم الجسيمات وكذلك ايجاد سطح البلازمون الرنيني(SPR) . كان قمة البلازمون الرنيني لجسيمات الفضة حوالي 402nm ولجسيمات النحاس النانوية 636nm . بينما كانت هناك قمتين للبلازمون الرنيني. لAg/Au(لب/قشرة) حيث كانت عند (406–516nm) ولCu/Au (لب/قشرة) كانت هناك قمة واحدة عند 565nm وذلك لكون قمة النحاس والذهب قريبة من بعضها . شكل وحجم الجسيمات النانوية تم تاكيدها بواسطة المجهر الالكتروني النافذ ذو الدقة العالية حيث كانت معدل حجم الجسيمات للفضة هي 12nm ولجسيمات النحاس 14nm وكان الحجم

*Email: dr.issamiq@gmail.com

حوالي 11nm لـ Au /Ag (لب/قشرة) بينما كانت ل Au/Cu (لب/قشرة) هي 13nm .فحص جهد زيتا (Zeta potential) اثبت ان جسيمات الفضة النانوية اكثر استقرارا (−23.11mV) من بين العناصر النانوية للمعادن بينما كانت للمركب Au/Ag (لب/قشرة) اكثر استقرارا (−27.77mV) بالمقارنة مع Au/Cu (لب/قشرة) النانوية.

Introduction

The synthesis of bimetallic nanoparticles has become so important in present times due to its diverse applications of nanotechnology. Particularly most of the bimetallic nanoparticles are focused to use in catalysis, plasmonic, magnetic, sensors, and many other applications. Colloidal dispersions of bimetallic nanoparticles have garnered a lot of attention in recent years, particularly in the areas of optoelectronic applications and catalysis [1-5].

Bimetallic nanoparticles (BMNP) have excelled monometallic nanocrystals owing to their improved electronic, optical and catalytic performances [6-8]. Nano-size Au particles have attracted lots of attentions due to their superior physical and chemical properties which are applied in many fields such as optical [9], catalysts [10], and biomedical materials [11]. There are notable synthesis methods [12-15] to control size and structure of Cu, Ag and Au nanoparticles, as these geometric factors are considered to significantly affect their properties. In this part, we only discussed the spherical structures of Cu, Ag /Au and their core/shell.

In Cu, Ag/Au case, the bulk Cu, Ag and Au are soluble at all compositions. But the structure of Cu, Ag/Au nanoparticles depends on the preparation methods. The structure might be the core shell, alloys or other morphology. Energetically favoring core/shell structure is with Au covering the core of Cu, Ag whose reverse core/shell structure is not stable and may transform back at a certain temperature. [16].

The Advantages of Au shell according to lots of the benefits from the core-shell nanoparticles, we proposed that Cu/Au and Ag/Au core-shell nanoparticles can achieve high activity and stability as well by controlled well on their geometric and electronic properties. The inner core can increase the amount of Au and provide large surface area. This technique is used not only for bio-applications [10, 17] but for electrochemical reaction observations [18-20].

In this paper we used the method of pulse laser ablation and also called dispersion method to prepare mono metallic Cu, Ag, Au and bi-metallic Cu/Au, Ag/Au core/shell nanoparticles, it is removal of material from a solid target by incidence of laser light. The Zeta potential (ZP) utilizes to determine the stability of colloidal and the magnitude of the zeta indicate the degree of electrostatic between similar charged particles in dispersion.

Experimental work

Cu, Ag and Au nanoparticles were produced by laser ablation of a Cu, Ag and Au targets (diameter = 1.5 mm, thickness = 0.5 mm, 99.99% immersed in a vessel filled with 5 mL of distill water (DW). The target irradiated vertically by a Q-switched Nd- YAG laser (DIAMOND-288 pattern EPLS), with wavelength (λ = 1064 nm) duration time at 6 Hz. The laser beam was focused by a focal length 12cm), subsequently, we put the pure solution with different metals and re-irradiating by pulsed Nd-YAG laser, the spot diameter of the focused laser beam was 4 mm. The experimental setup is shown schematically in Figure-1.

The UV-Vis absorption spectra of colloids were recorded by a spectrometer (type –Metertech SP-8001). A high resolution transmission electron microscope HRTEM (CM 30, Philips-Germany) was employed to study the structure of nanoparticles and to know the size of nanoparticles. The crystalline structure was examined by X-ray diffractions using (Philips PW) X-ray diffractometer system .The zeta potential measurement were carried out using a Zeta Plus (Brookhaven Instruments Corporation ,USA).

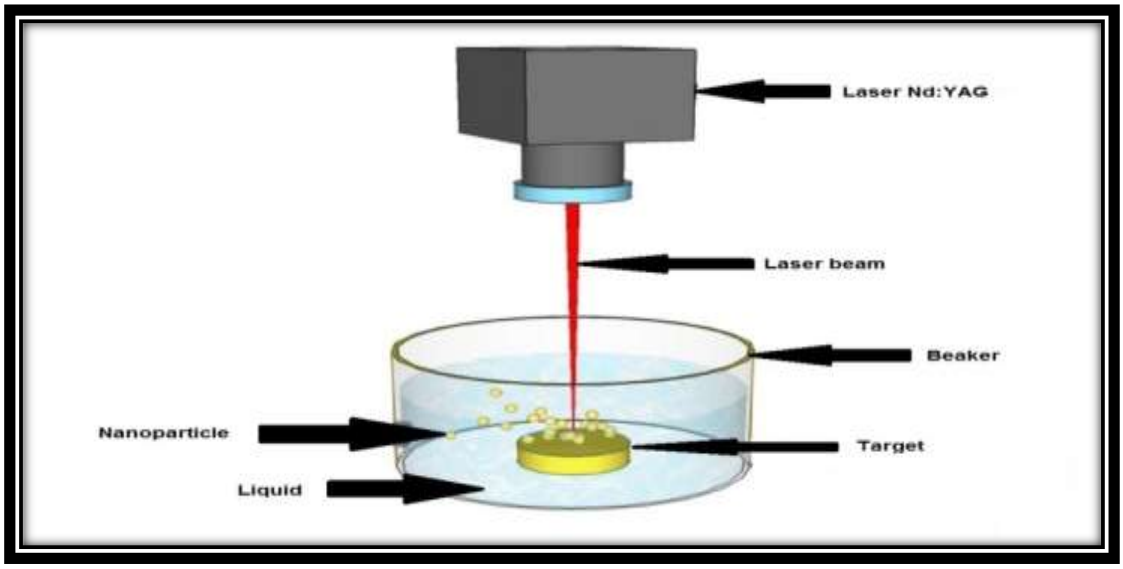

Figure 1-Pulse laser ablation in liquid system.

Results and Discussion

Absorption of Metals and Core-Shell Nanoparticles

Figures- (2, 3) show the absorbance spectra of Ag, and Cu NPs, by used laser power 400mJ and 200 pulses. The individual colloids, shows the surface Plasmon peaks (SPR) corresponding to the monometallic counter parts. The SPR peak position is at (402nm), (636nm) of Ag and Cu NPs respectively.

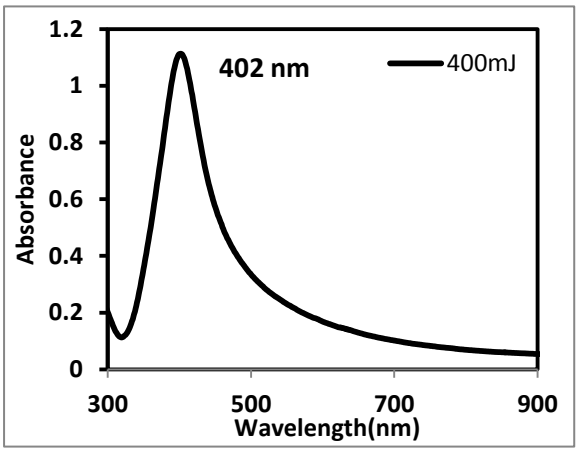

Figure 2- Optical absorption as a function of wavelength for Ag NPs

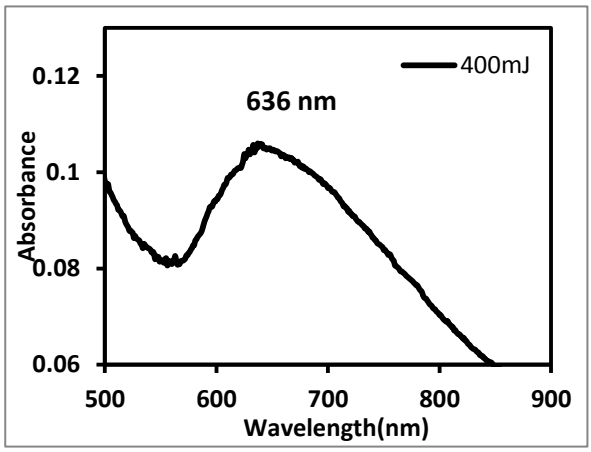

Figure 3-Optical absorption as a function of wavelength for Cu NPs

Figures- (4, 5) report the extinction spectra of Ag/Au core/shell and Cu/Au core/shell respectively. The Plasmon band is blue-shifted with mixed core/shell of Ag/ Au, this is may be due to the re-irradiation of Ag colloid during gold nanoparticles preparation causes of the duplicated division of Ag and Au nanoparticles. A physical mixture of the individual colloids, however, shows two surface Plasmon peaks corresponding to the monometallic counter parts. Formation of bimetallic dispersions depends on the kinetics and thermodynamics of reduction of individual components. The stability value for Au is expected to be close to that of silver for complete formation of the Ag/Au metallic colloid [21]. It is observed that both the metals are present with an enrichment of Au on the surface which it is clear in the second peak of Figure- 4. For Cu/Au core/shell nanoparticles Figure-5 indicating one peak appeared close to the two regions of Cu and Au. The SPE reduced and the one peak at 560 nm appeared because of the proximity of regions.

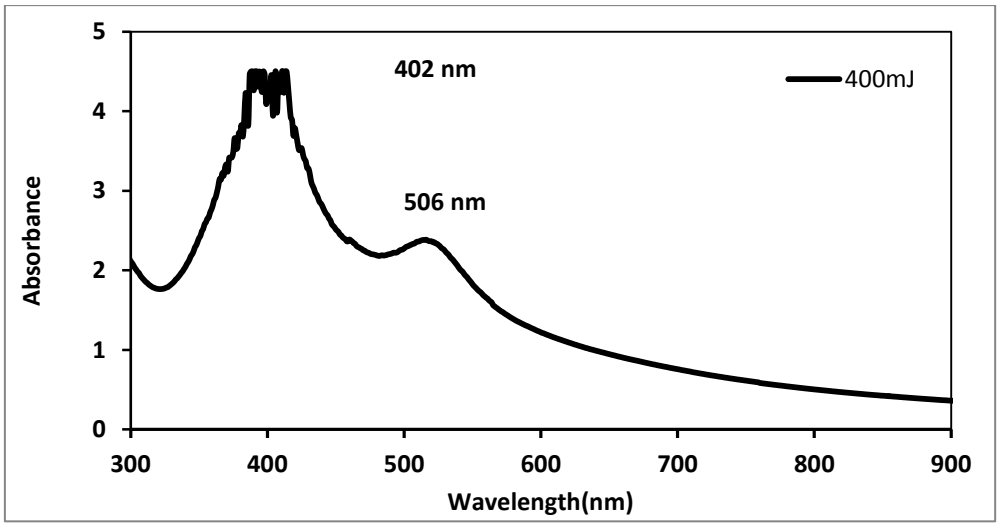

Figure 4- Optical absorption as a function of wavelength for Ag/Au NPs.

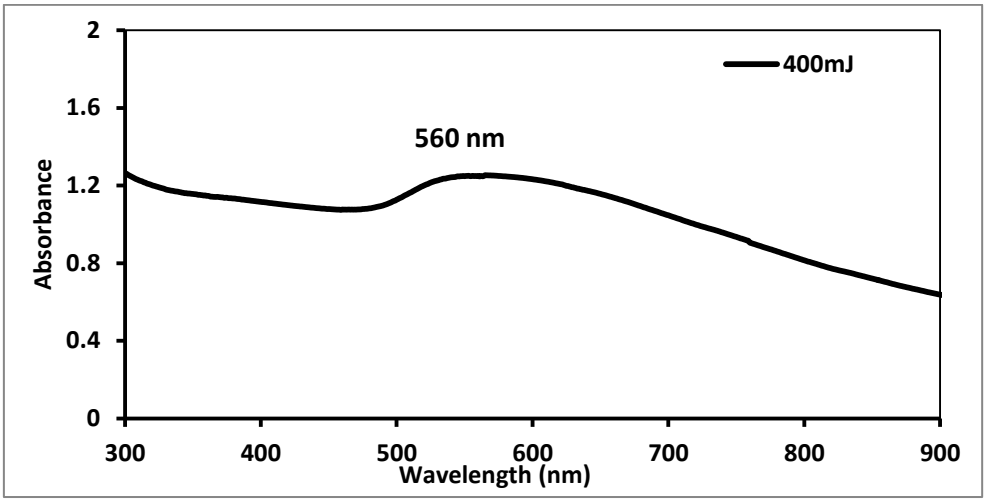

Figure 5-Optical absorption as a function of wavelength for Cu/Au NPs.

X-Ray diffraction analysis

Figure-6 shows the structure of Ag NPs which has a polycrystalline structure and cubic phase. The (111), and (200) planes which located that peaks at (2θ=37.93°, 44.03°) for Ag NPs agreement with the JCPDS standard card No. (#96-901-3049), Au and Ag have very similar lattice constants and hence their *d* and 2θvalues lie very close to each other except at 2θ =63.98° and 78.02° which corresponding to (220 and 311) for Au and Ag respectively. There is no lattice mismatch since the Au and Ag have very similar lattice parameters. In the case of Cu/Au core/shell all reflections are similar to monometallic Cu and Au nanoparticles. Figure-7 shows two a broad band at 42.47° and 49.41 (2θ) that can be attributed to the (111) and (200) crystallographic planes of Cu nanoparticles, the Cu NPs agreement with the JCPDS standard card No. (#96-901-3024). The peaks (111), (200),(220) and (311) planes that peaks at (2θ=38.20°,44.20° ,63.98° and 78.02°) for Au NPs which agreement with the JCPDS standard card No. 96-901-2431.

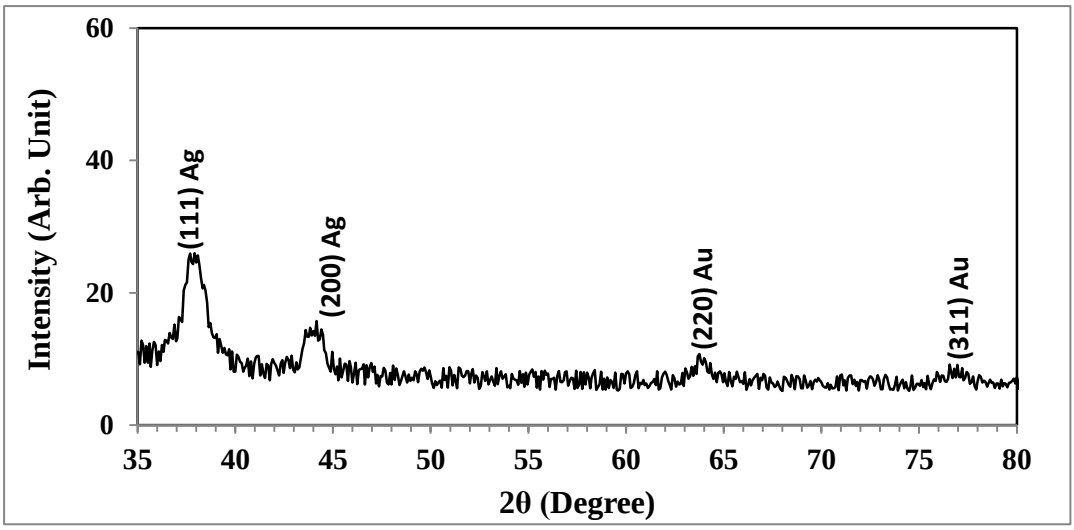

Figure 6- XRD Spectrum of Ag/Au NPs

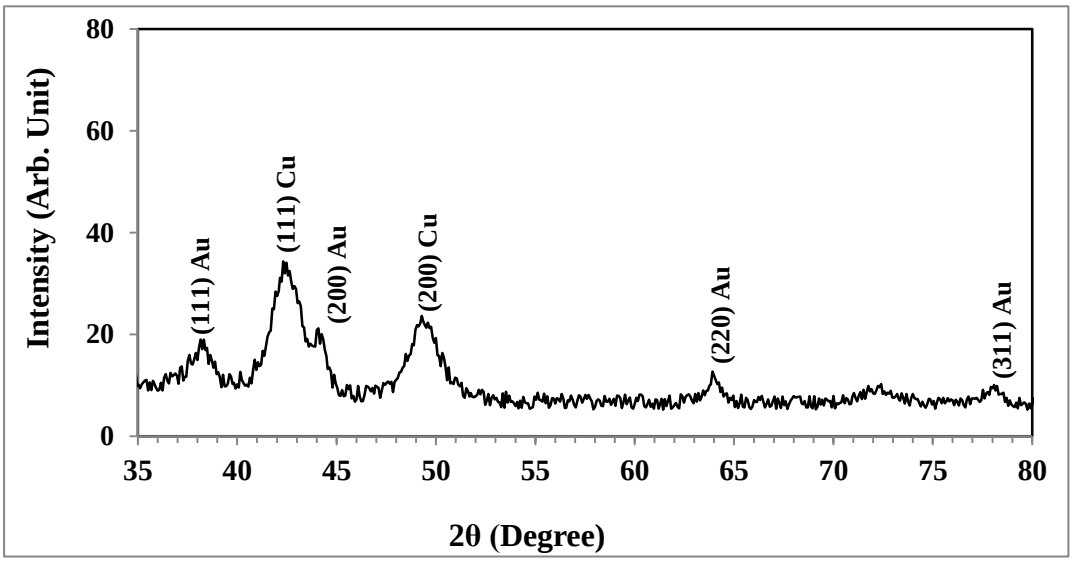

Figure 7- XRD Spectrum of Cu/Au NPs

2- HRTEM and Size Distribution of Ag, Cu and the core /shell NPs

The High Resolution Transmission Electron Microscopy (HRTEM) images were obtained for the samples in order to study the size distribution of the produced particles. Figures- (8, 9) show the histogram figures and size distribution of Ag and Cu NPs respectively, observed from these images that the average Ag NPs is around 12 nm, narrow distribution for Cu NPs that possess particle size around 14nm. Figures- (10-11) show the HRTEM images and size distribution of Ag/Au core/shell and Cu(core)-Au(shell) NPs respectively, where the average of Ag/Au core/shell NPs is around 11 nm, and average size is around 13nm for Cu/Au core/shell NPs. It is clear that the smallest particles are obtained for Au/Ag, but in all the cases we found aggregates smaller than 15 nm.

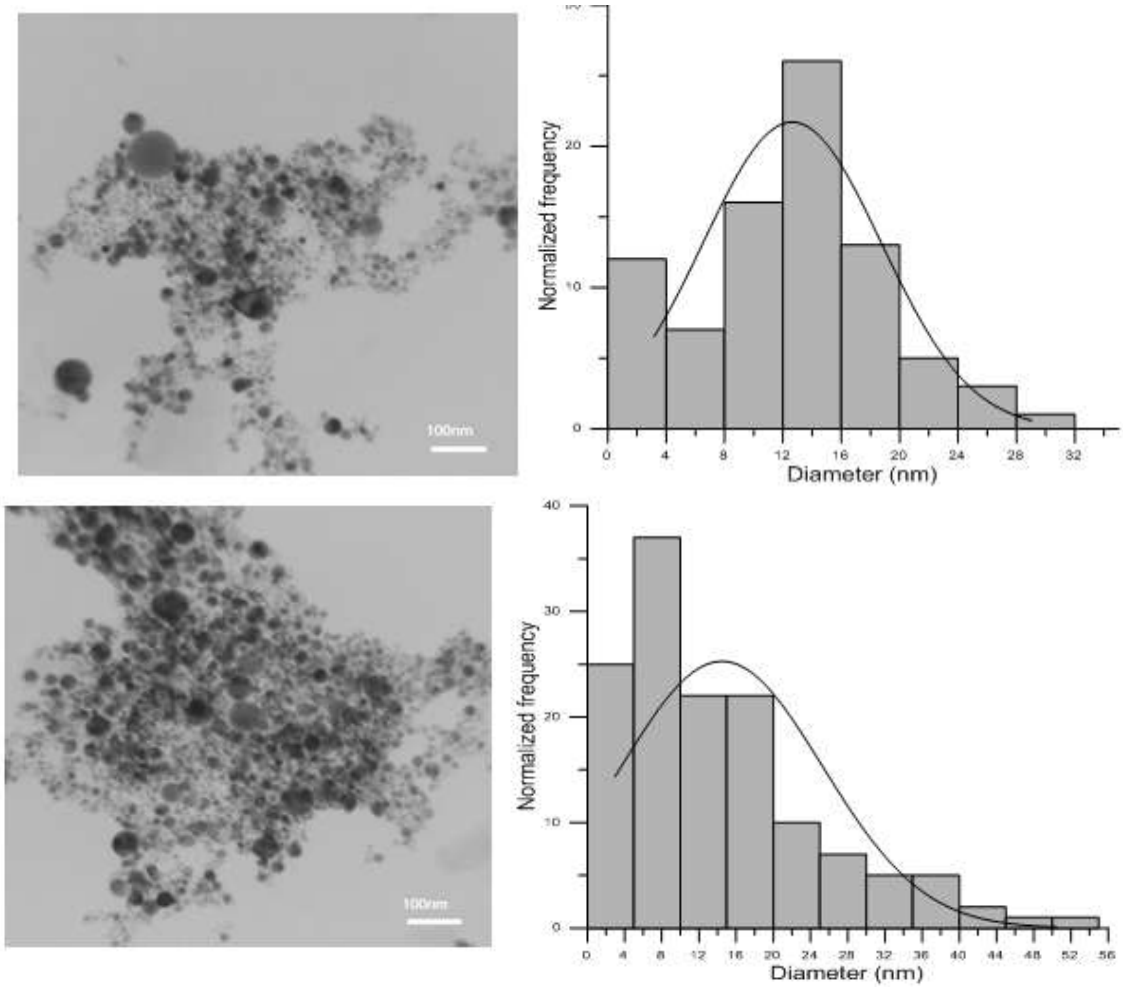

Figure 9-HRTEM image and size distribution of Cu nanoparticles

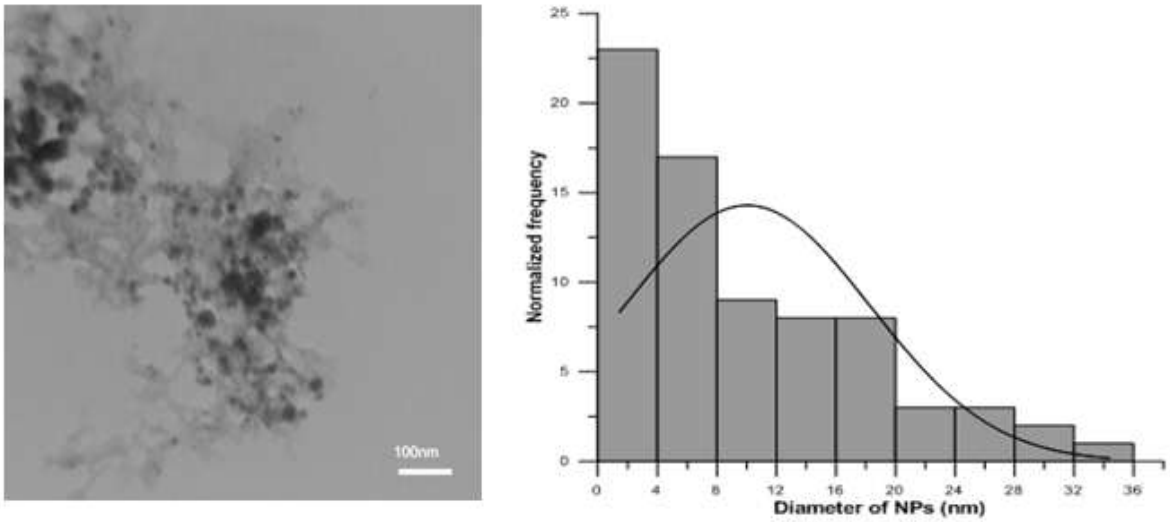

Figure 10- HRTEM image and size distribution of Ag/Au core/shell nanoparticles

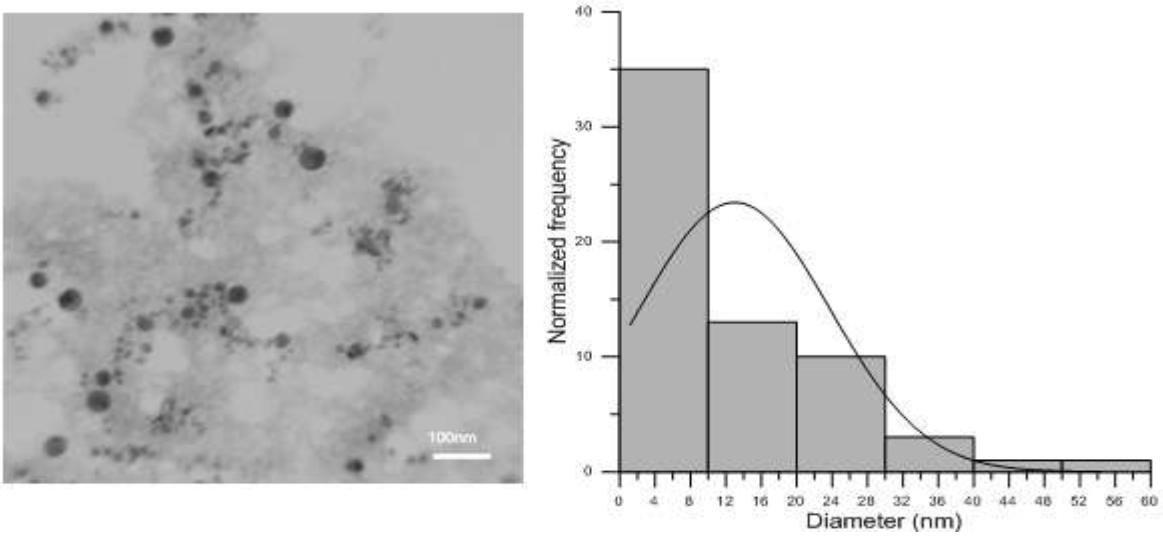

Figure 11- HRTEM image and size distribution of Cu/Au core/shell nanoparticles.

4- Stability of Nanoparticle Solution

It is well known that in practice the different configurations of nanoparticles coexist in a sample because not in all of the cases the clusters would be in the minimized energy configurations [22]. However, an important parameter that are included in this study is the atomistic distribution of the elements, inducing a significant difference on the electronic structure, which has a direct influence over the chemical and physical properties, as can be observed by a simple inspection of frontier orbital distributions (and values) for Ag/Au core/shell and Cu/Au core/shell structures. Figures- (12 and 13) show the results of Zeta potential measurements for the minimized energy configurations of Ag, Cu and Ag/Au , Cu/Au core shells. The figures include the geometry optimized model and the corresponding electrostatic potential distribution for the structures: Ag and Cu nanoparticles, Ag/Au and Cu/Au core shells, zeta potential values of Ag, and Cu NPs is -23.11mV, -22.27mV respectively. Results indicate the silver nanoparticle is more stability of others metals nanoparticles. Figure- (13) shows zeta potential values of colloid Ag/Au core/shell and Cu/Au core/shell which are -27.77mV and -17.28mV respectively. Note when mixed the noble metal (core/shell) dominant of stability Ag/ Au core/shell as shown in their values, while the results indicated lower formats coverage at the same applied potential for the Cu/Au core/shell nanoparticles than the Cu nanoparticles, suggesting an efficient removal of these intermediates probably due to the strong electronic coupling within these nanoparticles.

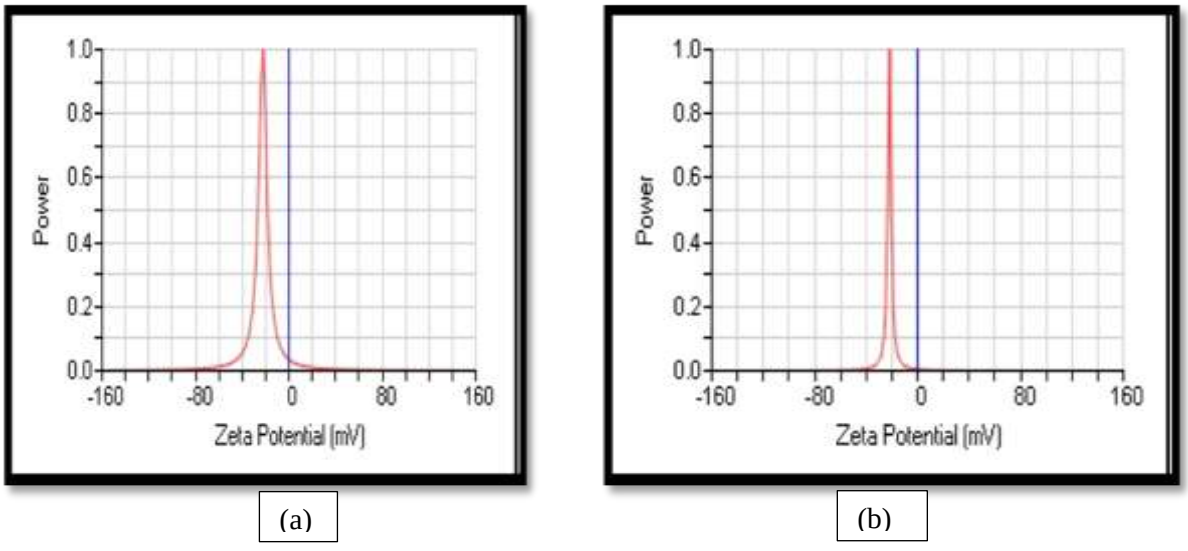

Figure 12- Zeta potential of stability in DI water of (a) Ag NPs (b) Cu NPs.

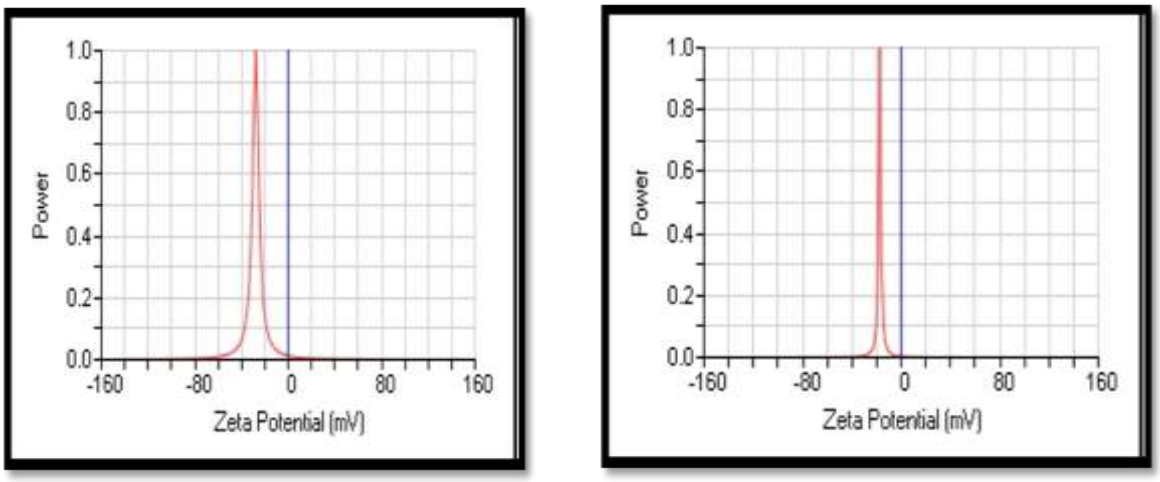

Figure 13- Zeta potential values of colloid (a) Ag/Au core/shell (b) Cu/Au core/shell

Conclusions

distilled water. HRTEM images proved the Nano size for these pure noble metals NPs and core-shell metals NPs with spherical shape. From ZP results show that the colloidal of Ag NPs is the most stabilizing than other noble metals, While Ag/Au core/shell is the most stabilizing than other core/shell metals NPs and Cu/Au core/shell is the most aggregation. Coating these nanoparticles with gold nanoparticles as a shell makes them useful in medical applications for getting high heat capacity that enables them absorb CO_2 laser that used in the field of cancer therapy.

References

1. Radha, N. **2010.** Recent Advances in Noble Metal Nanocatalysts for Suzuki and Heck Cross-Coupling Reactions. *Molecules*, **15**: 2124-2138**.**
2. Isam, M., Ahmed, K., and Dalya, K. **2016.** Synthesis and Zeta potential of Nobel metals (Pt,Au,Ag AND Cu)nanoparticles prepared by pulse laser ablation, *Sci. Int.(Lahore)* **28**(5): 4371-4375.
3. Landon, P., Collier, P. J., Papworth, A. J., Kiely, C.J., and Hutchings, G. J. **2002**. Direct formation of hydrogen peroxide from H_2/O_2 using a gold catalyst, *Chem. Commun*, **18**: 2058-2059.
4. Edwards, J. K., Selsone, B.E., Landon, P., Carley, A.F., Herzing, A., Kiely, C.J., and Hutchings, G. J. **2005**. Direct synthesis of hydrogen peroxide from H_2 and O_2 using TiO_2-supported Au–Pd catalysts. *J. Catal*, **236**: 69-79**.**
5. Vinodgopal, V., Yuanhua, He. , Muthupandian Ashokkumar, and Franz Grieser **2006**. Sonochemically Prepared Platinum−Ruthenium Bimetallic Nanoparticles. *J. Phys. Chem. B.*, **110** (9): 3849–3852.
6. Venkatesan, P. and Santhanalakshmi**,** J. **2012**. Synthesis and Characterization of Surfactant Stabilized Trimetallic Au-Ag-Pd Nanoparticles for Heck Coupling Reaction**.** *Physical Chemistry*, **2**(1): 12-15.
7. Megan, S. , Kevin, E., Mia Hall, Jamie, R. , Qiao Chen, and Christopher, C. **2014**. Synthesis and Catalytic Activity of Plutonic Stabilized Silver-Gold Bimetallic Nanoparticles. *RSC Adv*. **4**(94): 52279–52288.
8. Manavi, K., Kriti, S. , Bhavleen, K., and Kanchan, K. **2015 ,** Metal nanoparticles: Synthesis, characterization, toxicity and regulatory aspects. *Innovations in Pharmaceuticals and Pharmacotherapy***, 3** (4): 692-709.
9. Gotz, M., and Wendt, H. **1998,** Binary and ternary anode catalyst formulations including the elements W, Sn and Mo for PEMFCs operated on methanol or reformate gas. *Electrochim. Acta*, **43**:3637-3644.
10. Haruta, M. **2004,** Gold as a novel catalyst in the 21st century: Preparation, working mechanism and applications**.***Gold Bulletin*, **37**: 27-36.

11. Chen, J., Li, Z. Y., Au, L., Hartland, G.V. and Li, X. **2006**. Gold nanostructures: engineering their plasmonic properties for biomedical applications**.** *Chemical Society Reviews*, **35**:1084-94
12. Zhao, P. L., Astruc, D. **2013**. State of the art in gold nanoparticle synthesis. *Coordination Chemistry Reviews*, **257**: 638-65.
13. Brust, M., Wallker, M., Bethell, D., Schiffrin, D. J., and Whyman, R. **1994**. Synthesis of thio-derivatised gold nanoparticles in a two-phase liquid-liquid system. *Journal of the Chemical Society, Chemical communications*.**7**: 801-802.
14. Grzelczak, M., Perez-juste, J., Mulvaney, P., Liz-Marzan, L.M. **2008**. shape control in gold nanoparticle synthesis. *Chemical society Reviews.***104**: 293-346.
15. Ziegler, C. and Eychmuller, A. **2011**, Seeded Growth synthesis of uniform gold nanoparticles with diameters of 15-300 nm. *J.Phys Chem. C.* **115**(11):4502-4506.
16. Ascencio, J.A., Liu, H.B., Pal, U., Medina, A., and Wang, Z.L. **2006.** Transmission electron microscopy and theoretical analysis of Au-Cu nanoparticles: Atomic distribution and dynamic behavior, *Microscopy Research And Technique*, **69** : 522–530.
17. Senguptaa, A., Laucksb, M.L., Dildineb, N., Drapalab, E., Davis, E.J. **2005**. Bioaerosol characterization by surface-enhanced Raman spectroscopy (SERS). *Journal of aerosol science*, **36**: 651-64.
18. Yang, Z., Li, Y., Li, Z., Wu, D., Kang, J., and Xu, H. **2009**. Surface enhanced Raman scattering of pyridine adsorbed on Au/Pd core/shell nanoparticles**.** *The Journal of Chemical Physics***, 130**: 234705-7.
19. Chen, Y., Lim, H., Tang, Q., Gao, Y., Sun, T., and Yan, Q. **2010**. Solvent-free aerobic oxidation of benzyl alcohol over Pd monometallic and Au–Pd bimetallic catalysts supported on SBA-16 mesoporous molecular sieves**.** *Applied Catalysis A: General*, **380**: 55-65.
20. Duan, S., Fang, P. P., Fan, F. R., Broadwell, I., Yang, F. Z., and Wu, D. Y. **2011**. A density functional theory approach to mushroom-like platinum clusters on palladium-shell over Au core nanoparticles for high electrocatalytic activity. *Physical Chemistry Chemical Physics*, **13**: 5441-9.
21. Afzal, Sh., Latif, R., Rumana, Q., and Zia, R. **2012**. Synthesis, Characterization and Applications of Bimetallic (Au-Ag, Au-Pt, Au-Ru) Alloy Nanoparticles. *Rev.Adv.Mater. Sci*., **30**: 133-149.
22. Ahmed, K., Isam, M., and Dalya, K. **2016**. The Effect of Electric and Magnetic Field on Silver Nanoparticles Prepared by Pulse Laser Ablation. *International Journal of Scientific & Engineering Research*, **7**(6):976-980.